PHYSICAL REVIEW LETTERS

Fast-Ion Conduction and Flexibility of Glassy Networks

Deassy I. Novita and P. Boolchand

Department of Electrical and Computer Engineering, University of Cincinnati, Cincinnati, Ohio 45221-0030, USA

M. Malki

Centre de Recherche sur les Matériaux à Haute Température, CNRS, 1D Avenue de la Recherche Scientifique, 45071 Orléans, and Polytech'Orléans, Université d'Orléans, 8, rue Léonard de Vinci, 45072 Orléans, France

M. Micoulaut

Laboratoire de Physique Théorique de la Matière Condensée, Université Pierre et Marie Curie, Boite 121, 4, Place Jussieu, 75252 Paris, Cedex05, France

We observe two thresholds in the variations of electrical conductivity of dry $(AgI)_x(AgPO_3)_{1-x}$ solid electrolyte glasses, when the AgI additive concentration x increases to 9.5% and to 37.8%. Raman scattering complemented by calorimetric measurements confirms that these thresholds are signatures of the rigidity phase transitions at $x = 9.5\%$ from a stressed rigid to an isostatically (stress-free) rigid phase, and at $x = 37.8\%$ from isostatically rigid to a flexible phase. In the flexible phase, the electrical conductivity seems to increase as a power of x. This is in good agreement with the theoretical prediction based on 3D percolation.

The solid electrolytes, AgI, Ag_2S, Ag_2Se, exist in a noncrystalline or glassy phase, usually not as stoichiometric solids but as additives in base network glasses [1]. These additives can either segregate [1,2] as separate phases or uniformly mix [1] with the base glass to form homogeneous solid electrolyte glasses. Gaining a more complete understanding of ion transport in these systems is a basic scientific challenge, with important technological consequences. These materials find use in batteries, sensors, nonvolatile memories for portable devices [3], and electrochromic displays [4]. The $(AgI)_x(AgPO_3)_{1-x}$ solid electrolyte appears to form homogeneous glasses, and their physical behavior [5–7] including compositional variations in electrical conductivity [8,9] has been examined rather extensively, although a consensus on the data has been elusive. Here we show that the variability of the data is likely due to water contamination. Our work is on specifically prepared dry samples, and reveals physical properties displaying two thresholds, one near $x = 9.5\%$ and a second near $x = 37.8\%$. We show that these thresholds separate different elastic regimes in network structure.

Phase diagrams of disordered solids based on connectedness of their backbones have their origin in the simple and elegant ideas of mechanical constraints. The notion of constraints in mechanics was introduced by Lagrange [10], applied to understand mechanical stability of macroscopic structures by Maxwell [11], and to model elastic behavior of covalent glassy networks by Phillips and Thorpe [12]. That there are actually three (flexible, intermediate, and stressed-rigid) and not two (flexible and rigid) elastic phases of disordered solids is a more recent development [13–17] in the field that has opened new avenues to under-

stand the unfolding process of proteins [13], design of thin-film gate dielectrics for transistors [15], satisfiability problems in computational science [16], and the near absence of aging of covalent glassy networks [17] in intermediate phases. Our observations here bring electrolyte glasses under the same generic classification [18,19], and highlight network *flexibility* to be the functionality that promotes fast-ion conduction.

$AgPO_3$ possesses a glass a transition temperature [20] (T_g) of 254 °C, when synthesized by handling usual precursors in a *dry* [relative humidity (RH) $< 0.2\%$] ambient atmosphere. But T_g's of the glass decrease to the 160–190 °C range when precursors are handled in laboratory ambient environment (RH $\sim 50\%$) [8,9,20]. The role of bonded water in lowering T_g of a $AgPO_3$ glass was recognized earlier [21], although the highest T_g realized in the earlier work was only 189 °C. Present solid electrolyte glass samples were synthesized by weighing and intimately mixing 99.999% Ag_3PO_4, P_2O_5, and AgI as fine powders in a dry N_2 gas purged glove box [20] (RH $<$ 0.2%), and reacting them at 900 °C. Melts were equilibrated at 600 °C, and quenched on steel plates, and glass samples cycled through T_g to relieve frozen stress [20]. A model 2920 modulated-differential scanning calorimetry from TA Instruments operated at 3 °C/ min scan rate and 1 °C/100 s modulation rate was used to examine glass transitions [17]. A Solartron SI 1260 impedance spectrometer was used to study ac electrical conductivity [18] as a function of temperature in the 200 K $< T < T_g$ range, and frequency in the $1 < f < 106$ Hz range. Here we report on room temperature $f \rightarrow 0$ (dc) conductivity results. Raman scattering was excited using 514 nm radia-

tion, and the scattered radiation analyzed using a model T64000 triple monochromator system [17].

The observed variations in $T_g(x)$ and the nonreversing enthalpy, $\Delta H_{nr}(x)$, of present *dry* $(AgI)_x(AgPO_3)_{1-x}$ glasses are summarized in Figs. 1(a) and 1(b). Here x represents the mole fraction of AgI. We find $T_g(x)$ to monotonically decrease as AgI content increases, but the $\Delta H_{nr}(x)$ term to vary nonmonotonically displaying a rather striking global minimum (reversibility window [17]) in the $9.5\% < x < 37.8\%$ range. At higher x ($>45\%$), the $\Delta H_{nr}(x)$ term decreases again as glasses depolymerize. Variations in room temperature electrical conductivity, $\sigma(x)$, appear in Fig. 1(c), and show increases in steps, one near 9.5% and another near 37.8%. For comparison, we have shown in Figs. 1(a) and 1(c) variations in $T_g(x)$ and in $\sigma(x)$ reported by earlier groups [9,22,23]. The present findings on dry samples differ significantly from previous ones in the field.

The thermal and electrical results above lead to the obvious question, Are there vibrational anomalies associated with structure of these electrolyte glasses as were observed earlier in covalent systems [17,24]? This, indeed, is the case as revealed by our Raman scattering results (Fig. 2). The base glass is widely believed [20,25,26] to consist of chains of quasitetrahedral PO_4 units with each P atom having two bridging (O_b) and two terminal (O_t) oxygen near neighbors. In the base glass ($x = 0$), modes near 1140 cm^{-1} and 684 cm^{-1} are identified [20,25,26] with symmetric vibrations of P-O_t and P-O_b of these tetrahedra in polymeric chains. The asymmetric counterparts of these modes are weakly excited in Raman but strongly in IR [20,25,26]. And with increasing x, these modes steadily redshift and decrease in scattering strength as two new pairs of modes appear, one near 1000 and 750 cm^{-1}, and a second one near 960 and 720 cm^{-1}, and steadily grow in scattering strength. The first and second pair of modes are identified [26], respectively, with PO_4 tetrahedra present in small rings and large rings (Fig. 2). These results lead to a picture of these glasses as being chainlike at low x ($<30\%$), but becoming ringlike at high x ($>50\%$), features that are in harmony with decreasing molar volumes [6,27] and a loss of network connectivity independently supported by reduction of T_g's within the agglomeration theory [28]. Raman and IR [20] vibrational density of states change with glass composition, and these results are in contrast to earlier reports [23,27] that reveal little or no change.

The observed Raman line shapes when analyzed in terms of a superposition of Gaussians provide variations in frequency of the P-O_t symmetric mode near 1140 cm^{-1} [Figs. 2 and 3(a)]. The mode is found to steadily redshift displaying two vibrational thresholds, one near $x = 9.5\%$ and the other near $x = 37.8\%$, which correlate rather well with the walls of the reversibility window [Fig. 1(b)] and the steps in electrical conductivity. Redshift of the mode in question occurs as the interchain spacings increase due to
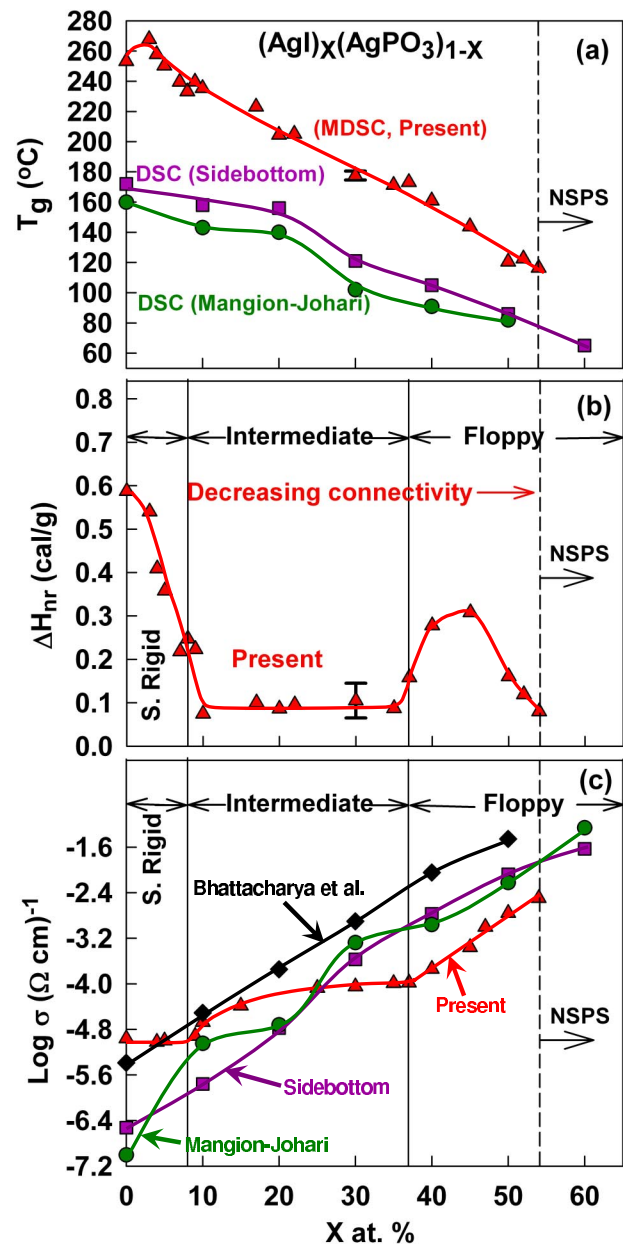

FIG. 1 (color online). Variations in (a) $T_g(x)$, (b) nonreversing enthalpy $\Delta H_{nr}(x)$, (c) room temperature conductivities, $\sigma(x)$ in dry $(AgI)_x(AgPO_3)_{1-x}$ glasses synthesized in the present work (red triangles) and those reported by Mangion-Johari (green circles) [22], Sidebottom (purple rectangles) [9], and Bhattacharya *et al.* (black diamond) [23]. At $x > 55\%$, T_g's decrease to near 65 °C, a value characteristic of AgI glass (see Ref. [1]). The reversibility window in $\Delta H_{nr}(x)$ fixes the intermediate phase, as in covalent glasses (see Refs. [18,24]).

insertion of AgI lowering the global connectivity of the backbone, a feature that has parallels in covalent glasses [17,24]. The underlying optical elasticity varies with glass composition as a power law, which is deduced by plotting the square of Raman mode frequency $[\nu^2 - \nu_c(1)^2]$ against glass composition $(x - x_c)$, and in the $0 < x < 9.5\%$ range,
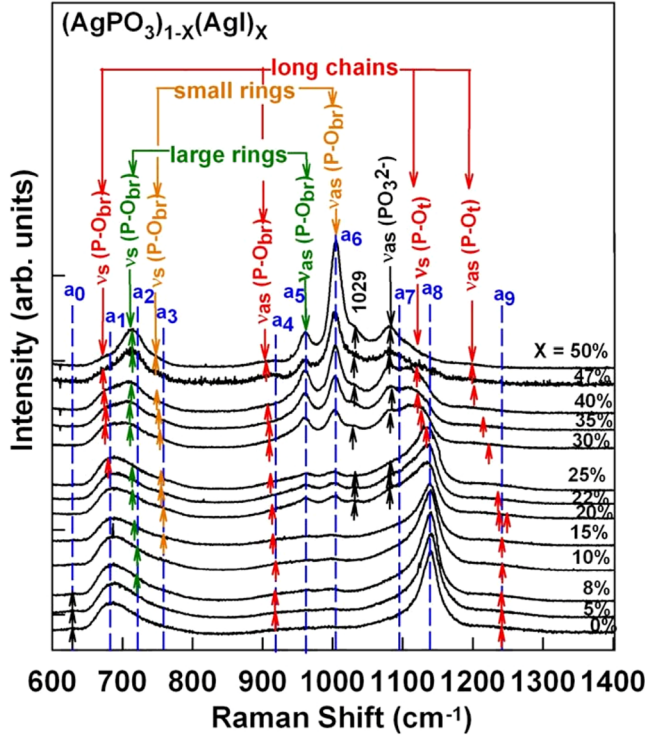
FIG. 2 (color online). Raman line shapes in *dry* $(AgPO_3)_{1-x} \times (AgI)_x$ glasses show vibrational modes as follows: a_1 (684.7 cm^{-1}) and a_4 (917.4 cm^{-1}) represent symmetric and asymmetric modes of P-O$_{br}$ in long chains, a_2 (722.8 cm^{-1}) and a_5 (967 cm^{-1}) represent symmetric and asymmetric modes of P-O$_{br}$ in large rings, a_3 (761.9 cm^{-1}) and a_6 (1004.6 cm^{-1}) represent symmetric and asymmetric modes of (P-O$_{br}$) in small rings, a_7 represents an asymmetric mode of PO$_3^{2-}$ species (Q_1 species) at 1095.1 cm^{-1}, and a_8 (1140 cm^{-1}) and a_9 (1245.4 cm^{-1}) represents symmetric and asymmetric stretch modes of P-O$_t$ in long chains. Glasses transform from chainlike to ringlike as the AgI content increases. The redshift of mode a_8 with x is analyzed in Fig. 3.

$$\nu^2 - \nu_c(1)^2 = A[x - x_c(1)]^{p_1}, \qquad (1)$$

and yields [Fig. 3(b)] the power law $p_1 = 1.25(2)$. Here $\nu_c(1)$ represents the value of ν at $x = x_c(1) = 9.5(3)\%$. The power law was deduced by plotting the $\log(\nu^2 - \nu_c(1)^2)$ against the $\log(x - x_c(1))$, with the slope of the line yielding p_1. In the $9.5\% < x < 37.8\%$ range, the corresponding power law is found [Fig. 3(c)] to be $p_2 = 0.98(3)$ with $x_c(2) = 37.8(5)\%$. As noted earlier, room temperature conductivities increase with x [Fig. 1(c)] to display a change in regime near $x_c(1) = 9.5\%$, and near $x_c(2) = 37.8\%$. If we fit the increase of conductivity at $x > x_c(2)$ to a power law,

$$\sigma(x) = B(x - x_c(2))^\mu, \qquad (2)$$

we obtain a value of $\mu = 1.78(10)$ and of $x_c(2) = 37.8(5)\%$ as shown in Figs. 1(c) and 3(d).

The thermal, optical and electrical results presented above lend themselves to the following interpretation.

The reversibility window, $9.5\% < x < 37.8\%$, in analogy to the case of covalent glasses [17,24], we identify with the intermediate phase of the present solid electrolyte glasses. The base AgPO$_3$ glass is weakly *stressed-rigid*, and AgI alloying steadily lowers the connectivity of the chain network as reflected in the reduction of $T_g(x)$ and emergence of the first sharp diffraction peak [5] near 0.7 A^{-1} in neutron scattering experiments. The Raman optical elastic power law of $p_1 = 1.25(2)$, for glasses in the $0 < x < 9.5\%$ range, is in reasonable accord with numerical predictions [29] for the power law in stressed-rigid networks ($p^{theo} = 1.4$), and the observed values of the elasticity power law in the stressed-rigid covalent glasses [17,24]. Taken together, the results show that glasses in the $0 < x < 9.5\%$ range possess backbones that are stressed-rigid, and that the threshold composition, $x_c(1) = 9.5\%$, represents the stress transition [14]. Currently, there are no theoretical estimates for the elastic power law in intermediate phases, but we note that the present value of $p_2 = 0.98(3)$ is in excellent agreement with the value observed in covalent glasses [17,24]. Thus, the reversibility window, Raman optical elastic thresholds, and elastic power laws show that glasses in the $0 < x < 9.5\%$ range possess backbones that are *rigid but mildly stressed*, in the $9.5\% < x < 37.8\%$ range these are *rigid but stress-free*, and in the $37.8\% < x < 55\%$ range these are elastically *flexible*. At higher x ($> 55\%$), glasses segregate into AgI-rich regions, as observed T_g's acquire values characteristic of AgI glass [1].

Addition of the electrolyte salt AgI to the insulating base AgPO$_3$ glass serves to provide Ag$^+$ carriers, and to also elastically soften the base glass. At low x ($<9.5\%$), Ag$^+$ ions undergo *localized* displacements in backbones as suggested by reverse Monte Carlo simulations [5], a view that is independently corroborated by intrinsically *stressed-rigid* character of these glasses in the present work. With increasing AgI, and particularly in the intermediate phase, backbones become stress-free [24] and Ag$^+$ displacements increase as do conductivities [Fig. 1(c)]. At higher x ($> 37.8\%$), backbones become elastically flexible and electrical conductivities increase precipitously as carriers freely diffuse [5] along percolative pathways. Thus, although carrier concentrations increase monotonically with x, the observed thresholds in $\sigma(x)$ suggest that it is network rigidity (flexibility) that controls fast-ion conduction by suppressing (promoting) Ag$^+$ ion migration.

The increase of ionic conductivity upon an elastic softening of a glass network represents an example of a complex system in which one functionality (elasticity) affects another (conductivity). The conductivity power law in the present glasses [$\mu = 1.78(10)$] is the same as found in $(K_2O)_x(SiO_2)_{1-x}$ glasses ($\mu = 1.77$) [18] when they become flexible. An electronic conductivity power law ($\mu = 1.60$) [30] and $\mu = 2.0$ [31] has been predicted in 3D bond depleted resistor networks once they percolate at the connectivity threshold. In summary, properties of flexibility and rigidity of glassy networks common place in covalent
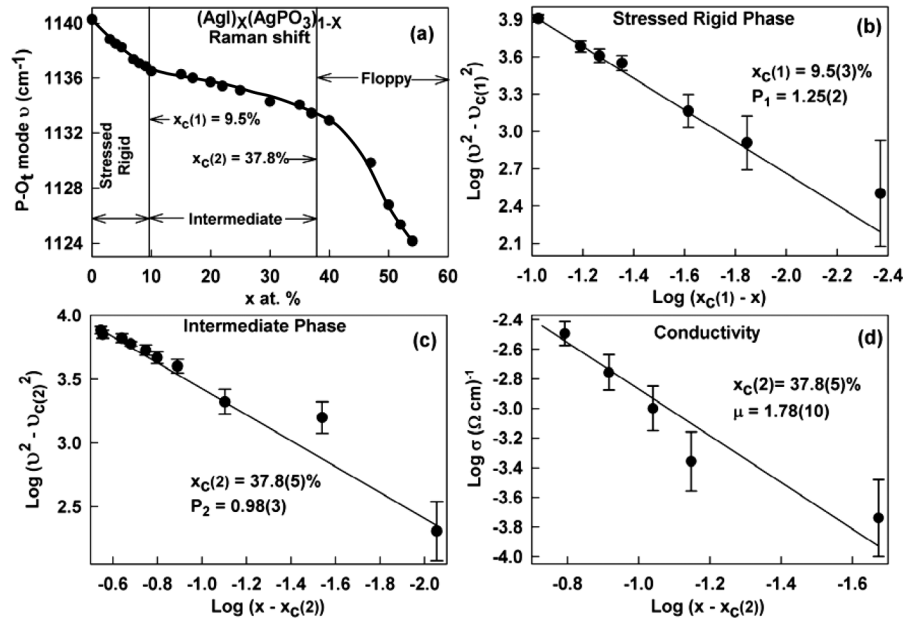
PHYSICAL REVIEW LETTERS

FIG. 3.   (a) Raman a_8 mode frequency redshifts with increasing x to display two thresholds, one near $x_c(1) = 9.5\%$ and a second near $x_c(2) = 37.8\%$. (b) Plot of $\log(\nu^2 - \nu_c(1)^2)$ against $\log(x_c(1) - x)$ in the $0 < x < 9.5\%$ range, and gives a slope $p_1 = 1.25(2)$. (c) Plot of $\log(\nu^2 - \nu_c(2)^2)$ against $\log(x_c(2) - x)$ in the $9.5\% < x < 37.8\%$ range and gives a slope $p_2 = 0.98(3)$. (d) Plot of $\log\sigma$ against $\log(x - x_c(2))$ and yields a conductivity power law $\mu = 1.78(10)$ in the flexible phase with $x_c(2) = 37.8\%$.

systems [14,17,24] apparently extend to solid electrolyte glasses as well, and fast-ion conduction is promoted when networks become flexible.

[1] P. Boolchand and W. J. Bresser, Nature (London) **410,** 1070 (2001).

[2] M. Mitkova, Y. Wang, and P. Boolchand, Phys. Rev. Lett. **83,** 3848 (1999).

[3] M. N. Kozicki *et al.*, Superlattices Microstruct. **34,** 459 (2003).

[4] M. Shizukuishi *et al.*, Jpn. J. Appl. Phys. **20,** 581 (1981).

[5] J. D. Wicks *et al.*, Phys. Rev. Lett. **74,** 726 (1995).

[6] J. Swenson and L. Borjesson, Phys. Rev. Lett. **77,** 3569 (1996).

[7] C. Angell, Annu. Rev. Phys. Chem. **43,** 693 (1992).

[8] M. Mangion and G. P. Johari, Phys. Rev. B **36,** 8845 (1987).

[9] D. L. Sidebottom, Phys. Rev. B **61,** 14 507 (2000).

[10] J. L. Lagrange, *Mecanique Analytique* (Desaint, Paris, 1788).

[11] J. C. Maxwell, Philos. Mag. **27,** 294 (1864).

[12] J. C. Phillips and M. F. Thorpe, Solid State Commun. **53,** 699 (1985).

[13] A. J. Rader *et al.*, Proc. Natl. Acad. Sci. U.S.A. **99,** 3540 (2002).

[14] M. Micoulaut and J. C. Phillips, Phys. Rev. B **67,** 104204 (2003); see also "Onset of Rigidity in Glasses: From Random to Self-Organized Networks," J. Non-Cryst. Solids (to be published).

[15] G. Lucovsky and J. C. Phillips, J. Non-Cryst. Solids **352,** 1711 (2006).

[16] J. Barre *et al.*, Phys. Rev. Lett. **94,** 208701 (2005).

[17] S. Chakravarty *et al.*, J. Phys. Condens. Matter **17,** L1 (2005).

[18] M. Malki *et al.*, Phys. Rev. Lett. **96,** 145504 (2006).

[19] G. N. Greaves and K. L. Ngai, Phys. Rev. B **52,** 6358 (1995).

[20] D. Novita and P. Boolchand (unpublished).

[21] P. Mustarelli *et al.*, J. Non-Cryst. Solids **163,** 97 (1993).

[22] M. B. M. Mangion and G. P. Johari, Phys. Chem. Glasses **29,** 225 (1988).

[23] S. Bhattacharya, D. Dutta, and A. Ghosh, Phys. Rev. B **73,** 104201 (2006).

[24] F. Wang *et al.*, Phys. Rev. B **71,** 174201 (2005).

[25] R. K. Brow, J. Non-Cryst. Solids **263,** 1 (2000).

[26] E. I. Kamitsos *et al.*, Phys. Chem. Glasses **36,** 141 (1995).

[27] J. P. Malugani and R. Mercier, Solid State Ionics **13,** 293 (1984).

[28] R. Kerner and M. Micoulaut, J. Non-Cryst. Solids **210,** 298 (1997).

[29] D. S. Franzblau and J. Tersoff, Phys. Rev. Lett. **68,** 2172 (1992).

[30] S. Kirkpatrick, Rev. Mod. Phys. **45,** 574 (1973).

[31] D. Stauffer and A. Aharony, *Introduction to Percolation Theory* (Taylor & Francis, Washington, DC, 1992).